ACS MEASUREMENT SCIENCE Au
AN OPEN ACCESS JOURNAL OF THE AMERICAN CHEMICAL SOCIETY

pubs.acs.org/measureau

Article

Dual "Static and Dynamic" Fluorescence Quenching Mechanisms Based Detection of TNT via a Cationic Conjugated Polymer

Arvin Sain Tanwar, Retwik Parui, Rabindranath Garai, Moirangthem Anita Chanu, and Parameswar Krishnan Iyer*

Cite This: *ACS Meas. Sci. Au* 2022, 2, 23–30

Read Online

ACCESS | Metrics & More | Article Recommendations | Supporting Information

ABSTRACT: A rare combination of dual static and dynamic fluorescence quenching mechanisms is reported, while sensing the nitroexplosive trinitrotoluene (TNT) in water by a cationic conjugated copolymer PFPy. Since the fluorophore PFPy interacts with TNT in both ground state as well as the excited states, a greater extent of interaction is facilitated between PFPy and the TNT, as a result of which the magnitude of the signal is amplified remarkably. The existence of these collective sensing mechanisms provides additional advantages to the sensing process and enhances the sensing parameters, such as LoD and highly competitive sensing processes in natural water bodies irrespective of the pH and at ambient conditions. These outcomes involving dual sensing mechanistic pathways expand the scope of developing efficient sensing probes for toxic chemical analyte and biomarker detection, preventing environmental pollution and strengthening security at sensitive locations while assisting in early diagnosis of disease biomarkers.

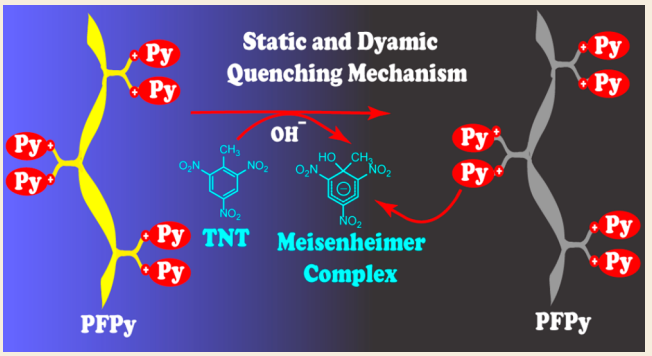

KEYWORDS: *Conjugated Polymer, Chemical Sensor, TNT, Explosives Detection, Fluorescence Quenching Assay*

INTRODUCTION

In recent years, research and development on sensing of explosives has gained tremendous attention.[1] 2,4,6-Trinitrotoluene (TNT) is a well-known nitroaromatic compound (NAC) belonging to a secondary class of explosives.[2] Due to its relatively high solubility in water, i.e., 130 mg/L at 20 °C, and its wide use in military operation, land mines, terrorism, and industrial applications, it contaminates land, agricultural soil, and water reservoirs and enters into the food chain.[3] Thus, it has been recognized by US Environment Protection Agency (EPA) as a contaminant, whose maximum permissible limit has been set to 20 μg/L in drinking water.[3] Its consumption causes severe health hazards, leading to skin irritation, liver function abnormalities, cataracts, cancer, and mutagenic activity post metabolism.[3] Additionally, other NACs, which possess a similar electron-deficient nature, generally interfere with selective detection of TNT. Hence, it is challenging to design a selective and sensitive TNT sensor from the view of the environmental pollution and overall security threat.

Thus far, few analytical techniques have been utilized for detection of TNT, for example, surface-enhanced Raman spectroscopy (SERS),[4] liquid chromatography–mass spectrometry,[5] electrochemical methods,[6] energy-dispersive X-ray diffraction,[7] and capillary electrophoresis.[8] Having their own distinct advantages, these techniques have certain limitations such as high instrument costs, low sensitivity, time-consuming process, and complications in on-site detection. However, fluorescence has been utilized widely in the sensing of explosive TNT due to its superior sensitivity, better selectivity, and rapid on-site detection with a variety of multiple portable economical platforms. Hence, various fluorescent probes have been designed for TNT sensing, which include carbon quantum dots, metal nanoparticles, organic nanoaggregates, and nonconjugated and conjugated polymers (CPs).[9−21]

CPs have been explored for sensing many vital analytes.[22,23] It is their remarkable photophysical properties such as tunable broad absorption, high photoluminescence (PL) quantum yield, and ultrasensitivity due to the "Molecular Wire Effect", which makes them ideal for sensing applications.[24] Hence, few CPs have been reported for TNT sensing.[15,16,25−27] Yet, many of them suffer from issues of sensitivity, selectivity, portability, and poor solubility in aqueous detection medium. Moreover, achieving a limit of detection (LOD) covering the safety limit of TNT in drinking water has also remained elusive.

Received: July 23, 2021
Published: September 8, 2021

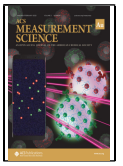

https://doi.org/10.1021/acsmeasuresciau.1c00023
ACS Meas. Sci. Au 2022, 2, 23–30

Scheme 1. (a) 1,6-Dibromohexane, Tetrabutylammonium Iodide (TBAI), 50% NaOH(aq.), 70 °C, 4 h. (b) Tetrakistriphenylphosphine Palladium (0), 2,1,3-Benzothiadiazole-4,7-Bis(boronic acid pinacol ester), aq. K_2CO_3, THF, reflux, 24 h; (c) Pyridine, DMF, 70 °C, 24 h

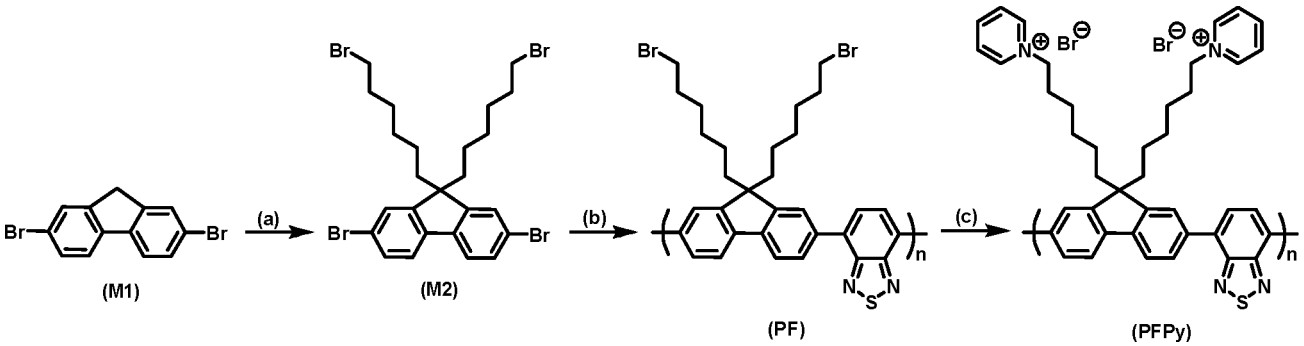

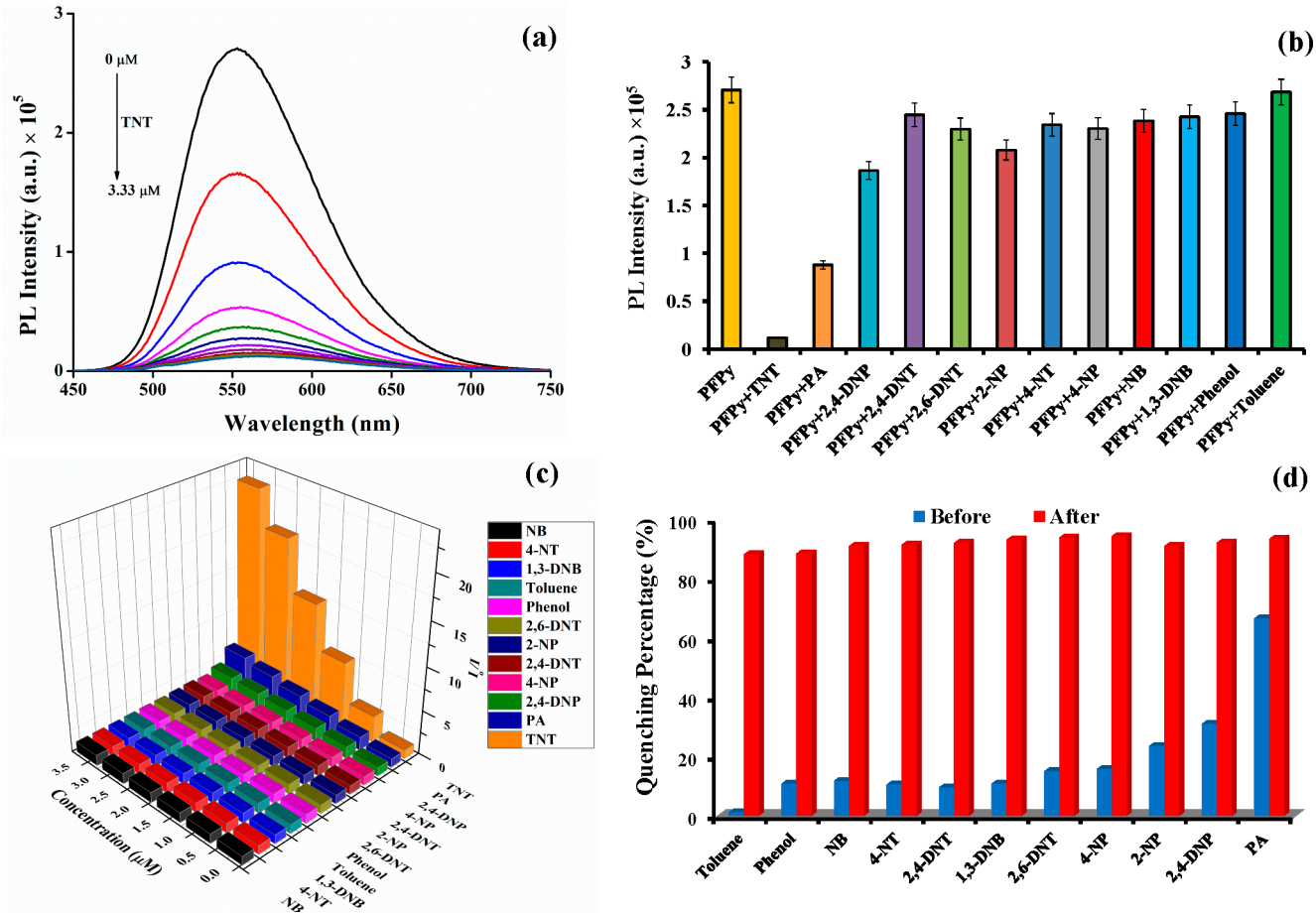

Figure 1. (a) PL spectra of PFPy (6.66 μM) at different concentration of TNT in water containing 10 mM NaOH. (b) Effect of various NACs (3.33 μM) on the PFPy (6.66 μM) intensity. (c) S–V plots (3D) obtained for various NACs. (d) Quenching (%) by various NACs (3.33 μM) before (blue) and after (red) addition of TNT (3.33 μM).

Herein, a cationic pyridinium appended fluorescent CP (PFPy) was synthesized for the specific and ultrasensitive detection of TNT in water (Scheme 1). In order to enhance the solubility of TNT, a strategy of using an alkaline medium (pH = 12) was used to facilitate the formation of the anionic Meisenheimer complex intermediate, which effectively undergoes electrostatic interaction with cationic side chains of the PFPy selectively even in trace levels and generates a detectable output rapidly. PFPy, an alternating copolymer of fluorene and benzothidiazole monomers, provides a desired red shift in the photophysical properties, and required essentially for realizing the energy transfer process with the anioinic Meisenheimer complex of TNT. The cationic side chains of the PFPy also behave as receptors, and binds very efficiently with the oppositely charged analyte species. A careful step-by-step elucidation and analysis of the sensing mechanism revealed the involvement of both static as well as dynamic quenching for TNT detection for the first time to the best of our knowledge. Thus, PFPy is a very unique sensor for TNT detection in water with exceptionally high sensitivity, stability, and good selectivity via combination of both static and dynamic

https://doi.org/10.1021/acsmeasuresciau.1c00023
ACS Meas. Sci. Au 2022, 2, 23–30

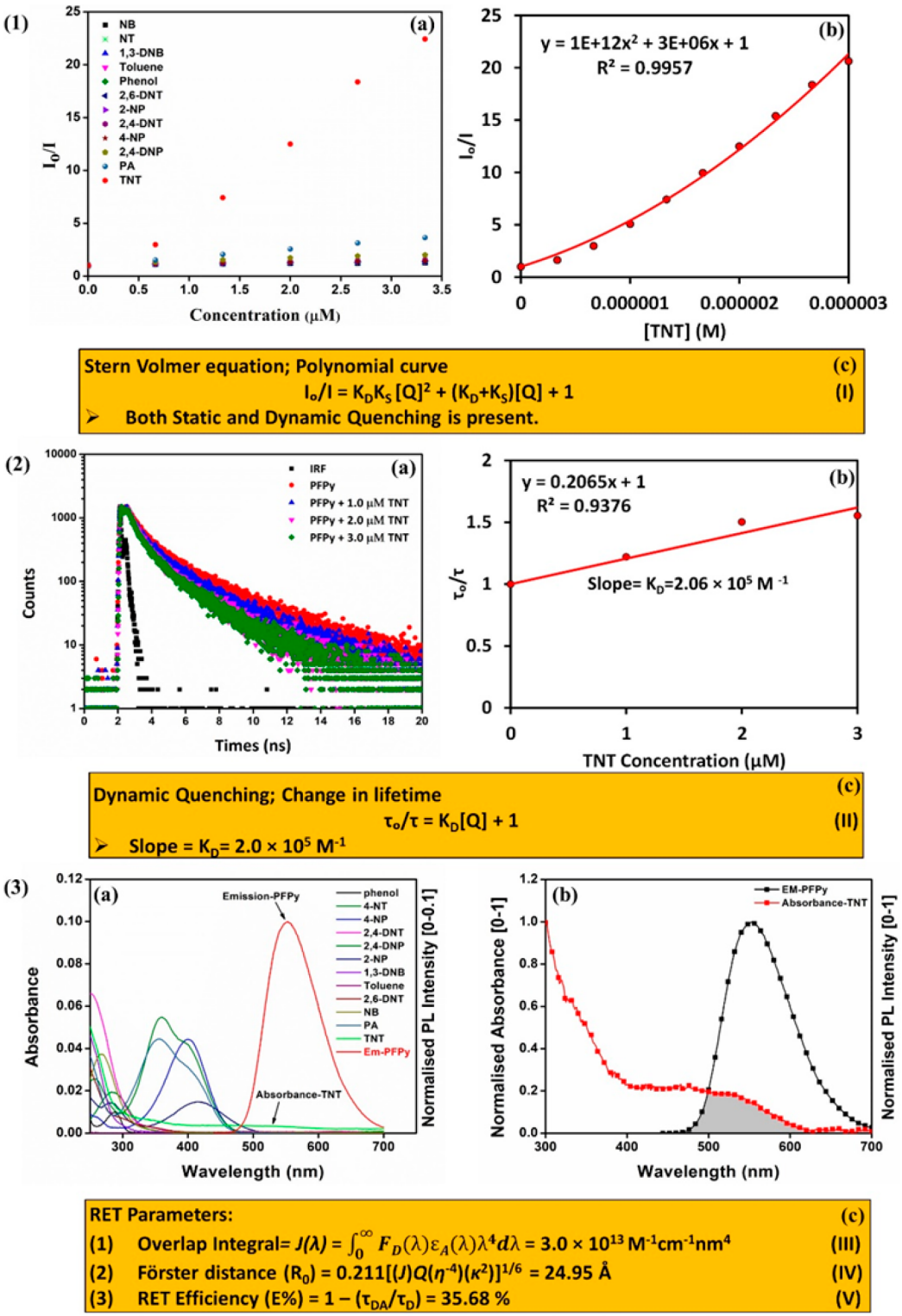

Figure 2. (1) Stern–Volmer (S–V) plot (2D) obtained for (a) all NACs and (b) second-order polynomial fitting of S–V plot for TNT. (c) S–V equation for both static and dynamic quenching. (2) (a) Time-resolved photoluminescence (TRPL) spectra of PFPy (6.66 μM) in the absence and presence of various concentration of TNT in water containing 10 mM NaOH. (b) Change in lifetime at various concentrations of TNT. (c) Equation (II) for dynamic quenching: where τ and τ_o are the average fluorescence lifetime with and without TNT, respectively. (3) (a) Spectral overlap between the normalized PL spectrum [0–0.1] of CP PFPy with absorbance of various NACs in water containing 10 mM NaOH. (b) Spectral overlapping region between the normalized emission spectrum of PFPy with TNT in water containing 10 mM NaOH. (c) Equations for RET parameters: (1) Equation (III)-where J denotes overlap integral value, $F_D(\lambda)$ represents the corrected fluorescence intensity from λ to $\Delta\lambda$ with total fluorescence intensity for PFPy normalized to 1, and ε_A represents molar absorptivity of acceptor in M^{-1} cm^{-1}. (2) Equation (IV)-where R_0 represents Förster distance, Q denotes the fluoresence quantum yield of PFPy, η represents refractive index of the medium, and k^2 signifies dipole orientation factor (0.667). (3) Equation (V)-where E% denotes RET efficiency, τ_{DA} and τ_D are the average fluorescence lifetime with and without quencher, i.e., TNT.

https://doi.org/10.1021/acsmeasuresciau.1c00023
ACS Meas. Sci. Au 2022, 2, 23–30

quenching mechanisms, providing high precision for TNT detection.

RESULTS AND DISCUSSION

Synthesis and Characterization of PFPy

The synthesis of the desired copolymer PFPy is depicted in Scheme 1. The products (monomer and polymer) at each step were purified and well characterized (Figures S1−S5). PF acts as a precursor polymer for PFPy synthesis. Cationic pyridinium units, that work as key receptor sites for the analyte TNT binding, also making it soluble in polar solvents (water, DMSO, etc.), were strategically linked to the pendant chains to generate the final copolymer PFPy. The aqueous solution of PFPy displayed a UV−vis absorption peak at 430 nm and emission peak at 553 nm (excitation wavelength = 430 nm) (Figure S6) with a remarkable fluorescence quantum yield (Φ_s) of 0.59 in water. The fluorescence emission peak (553 nm) obtained for PFPy at pH = 12 was monitored to evaluate the sensing response of PFPy toward TNT (Figure S7).

Sensing Studies for TNT Detection

The cationic PFPy copolymer was highly fluorescent as visualized under UV light even at a very dilute concentration (6.66×10^{-6} M) (Figure S8) and was found to be very sensitive and highly selective to TNT (Figure S9). The PL intensity of PFPy is quenched by ∼39% after the first addition of 0.33 μM TNT solution (Figure 1a) and reduces by ∼97% at 3.3 μM TNT solution (Figures 1a and S8). As a result of this extraordinary sensitivity of PFPy toward TNT, an LOD of 4.94 fM was achieved (Figure S10), which is the best reported value for TNT detection (Table S2).

Selectivity Studies

Selectivity has always been a huge challenge in the development of efficient sensor platforms. Especially for the detection of nitroexplosive TNT, its most identical chemical analogue picric acid (PA) interferes in its detection, as can be noticed in the previous reports (Table S2). Therefore, keeping the same experimental conditions that were optimized for the detection of TNT, selectivity studies of PFPy were performed with various common interfering analytes such as 1,3-DNB, 4-NP, PA, 2,4-DNT, 2,4-DNP, toluene, 4-NT, 2,6-DNT, NB, 2-NP, and phenol. It was found that PFPy possesses high selectivity only toward TNT (Figures 1b and S11). The Stern−Volmer (S−V) plots obtained for all the interfering NACs confirmed the quenching efficiency values for various NACs to be negligible compared to that of TNT (Figure 1c) confirming that PFPy has extraordinary selectivity toward TNT as established via studies performed in a competitive environment with different NACs.

Further, 2,6-DNT (3.33 μM) was mixed with the above PFPy (6.66 μM) solution, so that 2,6-DNT could interact with the PFPy prior to the additional mixing of TNT (3.33 μM). It was observed that adding 2,6-DNT (3.33 μM) to the solution of PFPy caused an insignificant change in the PL intensity, while TNT caused substantial quenching of fluorescence even in the presence of 2,6-DNT (Figures 1d and S12). Since TNT forms the intermediate anionic Meisenheimer complex rapidly compared to 2,6-DNT, it selectively binds the cationic pyridinium receptors of PFPy even in the presence of 2,6-DNT. Similar competitive studies were done with other NACs, and identical results were obtained, indicating high selectivity of the PFPy sensing system for TNT even in the presence of interfering competitive NACs (Figures 1d and S13−S22). These studies confirm that the PFPy polymeric system is an exceptional sensor that provides a very sensitive, selective, and rapid detection of TNT even in a competitive environment.

Mechanism of Sensing

To analyze the very high sensing performance of the PFPy, it was necessary to precisely understand the mechanism of sensing among the many possibilities.[22,28−30] On analyzing the S−V plot for TNT titration, the best fitting for a second order of the polynomial curve was observed [Figure 2 (1a and 1b)]. This second-order polynomial curve of the S−V plot is evidence for the coexistence of both static and dynamic quenching mechanisms in any sensing system [Figure 2(1c)].[31] In this polynomial equation (I) [Figure 2 (1c)], I and I_o are the PL intensities of the PFPy with and without TNT, [Q] denotes the concentration of the quencher, i.e., [TNT], K_D and K_S are quenching constants for the corresponding dynamic and static quenching, respectively. Second, to confirm the involvement of dynamic quenching in the sensing process and determine the corresponding value of K_D, TRPL studies of PFPy were performed at various concentrations of TNT and its fluorescence lifetime was monitored. Interestingly, there was a noteworthy decrease in the fluorescence lifetime of PFPy after addition of TNT (3.33 μM) [Figure 2 (2a) and Table S1]. This confirmed the presence of dynamic quenching during the sensing process.[28,31] Further, this change in fluorescence lifetime was plotted as τ_o/τ with respect to various concentrations of TNT [Figure 2 (2b)], where τ and τ_o are the average fluorescence lifetime with and without TNT, respectively. The linear fitting of the above plot (τ_o/τ vs [TNT]) yielded an equation of a straight line whose intercept is 1, and the slope of this equation represents the dynamic quenching constant (K_D), which was found to be 2.06×10^5 M^{-1} [Figure 2 (2b)].[31] This unusually high value of K_D specifies high fluorescence quenching efficiency due to the dynamic quenching mechanism.

Additionally, there are various subtypes of dynamic quenching mechanisms that exist, which are due to either collisional interactions or the involvement of excited-state phenomena such as Förster resonance energy transfer (FRET) in the sensing process. Generally, FRET has three primary conditions for occurring in any donor (D) and acceptor (A) sensing system. First, there should be significant overlap between the absorbance of the acceptor and the fluorescence of the donor. Second, the distance between the donor and the acceptor, i.e., the Förster distance, should be <10 nm for an effective FRET. Third, they should have suitable relative dipole orientations for FRET to occur.[28] To verify this, UV−vis absorption spectra of all the NACs and the normalized emission spectrum of the PFPy were plotted together [Figure 2 (3a)]. It was found that among all the NACs only TNT had an effective spectral overlap with the emission spectrum of PFPy [Figure 2 (3b)]. Hence, a very high selectivity was achieved for TNT as compared to other NACs. Further, RET parameters were also calculated for TNT sensing using the equations shown in Figure 2 (3c),[28] where J represents the overlap integral [Figure 2 (3c); equation (III)], which governs the extent of RET and was found to be 3.0×10^{13} M^{-1} cm^{-1} nm^4 (Table S3). The value obtained for the Förster distance (R_0) [Figure 2 (3c); equation (IV)], was found to be 24.95 Å, which also fits in between the range of feasible FRET to occur. RET efficiency for this sensing system was found to be 35.68%,

https://doi.org/10.1021/acsmeasuresciau.1c00023
ACS Meas. Sci. Au 2022, 2, 23−30

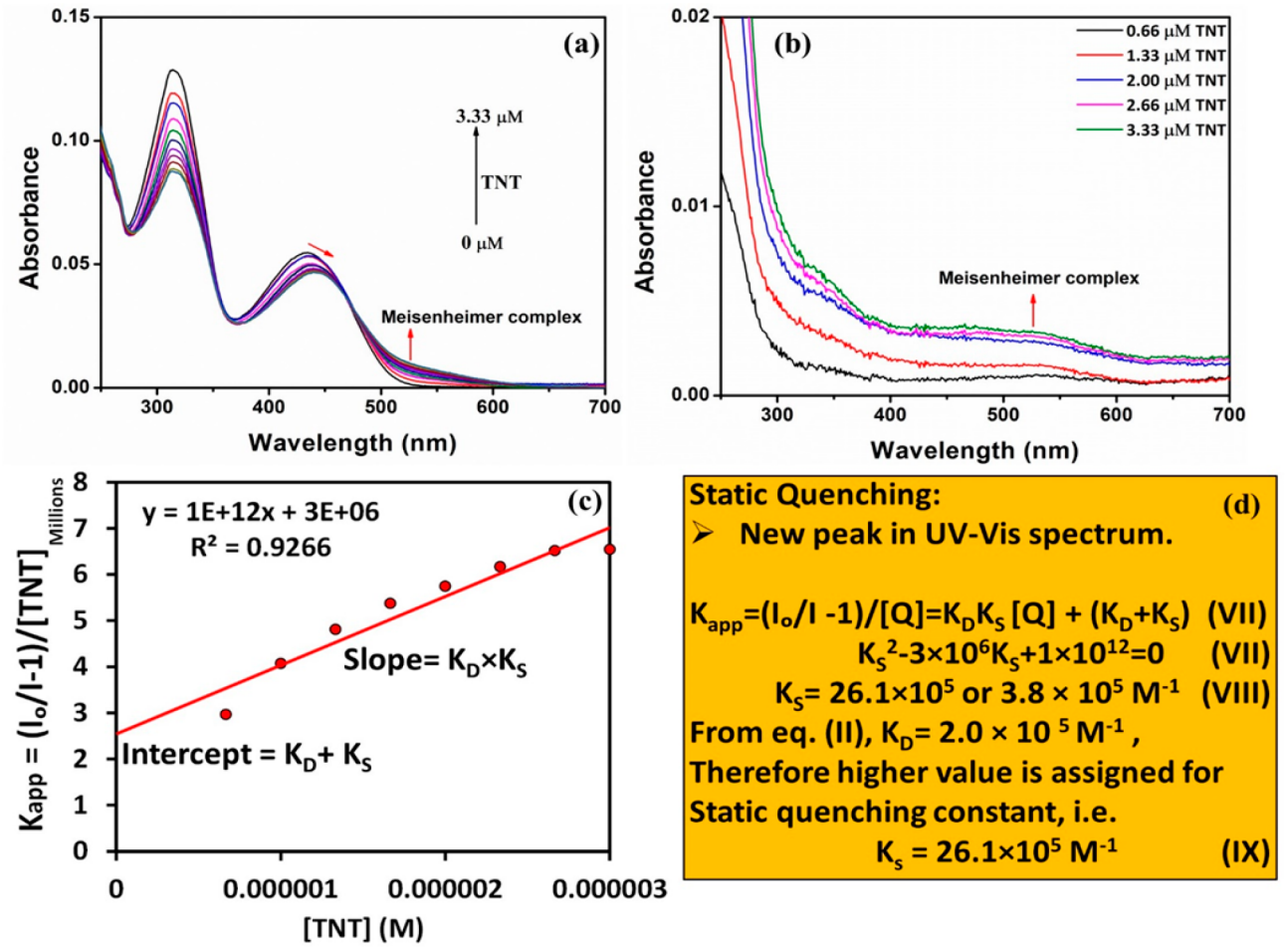

Figure 3. (a) Absorbance of PFPy (6.66 μM) in the presence of various amounts of TNT in water containing 10 mM NaOH. (b) Absorbance of TNT in water containing 10 mM NaOH. (c) Plot of K_{app} versus concentration of TNT in water containing 10 mM NaOH. (d) Equations and calculation for static and dynamic quenching constants, i.e., K_S and K_D, respectively.

which further confirms the contribution of RET in the mechanism of sensing [Figure 2 (3c); equation (V)]. Additionally, like the RET, inner filter effect (IFE) is also governed by the spectral overlap. However, in the case of IFE, spectral overlap happens among the emission and/or the excitation spectrum of fluorophore (PFPy) with absorbance of quencher (TNT).[22] Hence, to check if IFE is present, IFE corrections were performed using previously established methods via eq VI.[29,31,32]

$$I_{corr}/I_{obs} = 10^{(A_{ex}+A_{em})/2} \quad \text{(VI)}$$

where I_{corr} and I_{obs} signify PL intensities after and before IFE corrections, A_{ex} and A_{em} are the absorbance of the sensing system at the excitation and emission wavelength of the fluorophores, i.e., PFPy. It was found that there is no significant change in the PL intensity as well as in the suppression efficiency after performing the IFE correction [Figure S23 and Table S4 (detailed data are listed here)]. These results clearly exclude the involvement of IFE in the mechanism of TNT sensing.

Furthermore, to prove the involvement of static quenching (ground-state complexation) in the mechanism of sensing and to calculate its corresponding quenching constant (K_s), the absorbance of PFPy (6.66 μM) was obtained in the presence of various amounts of TNT (Figure 3a). It was seen that there is a shift in the absorption peak of PFPy to 440 nm. This shift in the peak of cationic PFPy clearly indicated the formation of ground-state complex with anionic Meisenheimer complex of TNT, while the appearance of a new absorption band at around 460 nm corresponds to the formation of the intermediate Meisenheimer complex of TNT at pH 12 (Figure 3b and Figure S24).[33,34] However, the anionic Meisenheimer peak was not observed in water at neutral pH, and hence, fluorescence quenching did not occur in water at neutral pH conditions (Figures S26 and S27). These key observations further prove the involvement of the static quenching mechanism in the sensing process. Additionally, in order to calculate the value of K_S, a plot of K_{app} versus concentration of TNT was obtained (Figure 3c). This curve was linearly fitted where the slope of this linear curve represents the ($K_D \times K_S$) value, which was 1×10^{12} M^{-2}, and the intercept of this line represents the ($K_D + K_S$) value, and was found to be 3×10^6 M^{-1} (Figure 3c). Rearrangement of the aforementioned values yielded a quadratic equations (VII), whose solutions are shown in equation (VIII), i.e., $K_S = 26.1 \times 10^5$ M^{-1} or 3.8×10^5 M^{-1}. Previously, from equation (II), the value of K_D, i.e., 2.0×10^5 M^{-1} was already known. Therefore, the higher value was assigned for the static quenching constant (K_S), i.e., 26.1×10^5 M^{-1} (Figure 3d, equation IX). The higher value of K_S clearly indicated the dominance of the static quenching in the mechanism of sensing and that was also responsible for higher

https://doi.org/10.1021/acsmeasuresciau.1c00023
ACS Meas. Sci. Au 2022, 2, 23−30

selectivity as well as ultrasensitivity of the PFPy sensing system for TNT.

Overall, PFPy possessed outstanding sensitivity and high selectivity toward TNT due to the strong static quenching mechanism along with remarkable dynamic quenching mechanism, which is exceptional and has been explored elaborately for the first time (Table S2). This combined dynamic and static quenching mechanism can be adopted to develop efficient fluorescent sensors, based on quenching of fluorophore via both collisional as well as complex formation with the same analyte/quencher. Interestingly, these results are very unique for an analyte/quencher like TNT. These collective sensing mechanisms can add extra advantage for enhancing the sensing parameters, such as LoD, competitive sensing, etc. As the fluorophore interacts with the quencher in both ground as well as excited states, this leads to a greater extent of interaction by the fluorophore with the analyte/quencher and hence the magnitude of signal is amplified remarkably (Figure 4).

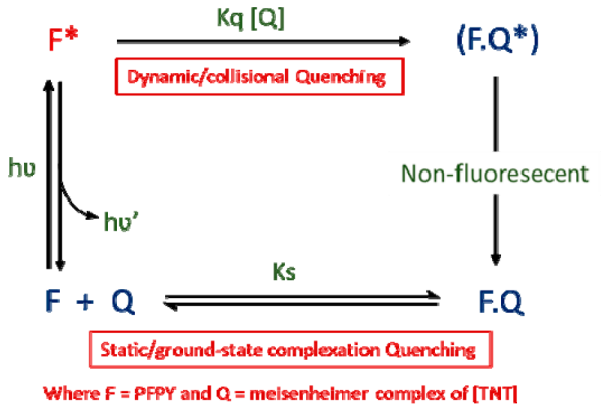

Figure 4. Combined dynamic and static quenching of the same population of the fluorophore PFPy via quencher (*Q*), i.e., Meisenheimer complex of TNT.

Detection of TNT in a Natural Reservoir

To further evaluate the feasibility of PFPy in an open water reservoir, different samples of water were obtained from the "Serpentine Lake" (inside IIT Guwahati campus). These samples were filtered through membrane of size 0.2 μm and then tested for TNT sensing. It was found that the water samples did not cause any substantial change in the intensity of the PFPy, confirming the absence of TNT. These samples were spiked with a known amount of TNT and then tested under the same conditions (Table 1). Recoveries were found to be high, i.e., in the range of 90−100% with very minor RSD values. Therefore, PFPy can be used to detect TNT efficiently in natural water reservoirs and their concentrations can be estimated using PFPy.

Table 1. Detection of TNT in Reservoir

reservoir	added (10^{-9} M)	found (10^{-9} M)	recovery (%)	RSD (%, n = 3)
Lake water	9.00	8.65	96.1	7.79
	15.00	14.20	94.6	2.67
	30.00	27.30	91.0	3.26

Sensing on Portable Testing Strips

For on-site contact-mode detection of TNT, a very simple methodology was adopted to prepare economical and convenient paper test device strips. For this purpose, Whatman filter paper (Grade I) was cut into a convenient size (1 cm × 1 cm) and desired shape (square in this case) and dipped into the PFPy solution (10^{-4} M) for solid-phase rapid on-site contact-mode detection. Subsequently, the paper devices were dried and then dipped in water containing 10 mM NaOH solution and further dried for final use for on-site detection of TNT. Fixed volumes (10 μL) of different concentrations of TNT solutions were spotted over the portable paper device strips, and fluorescence quenched marks were clearly observed on UV irradiation (Figure 5). The dark spots can be clearly

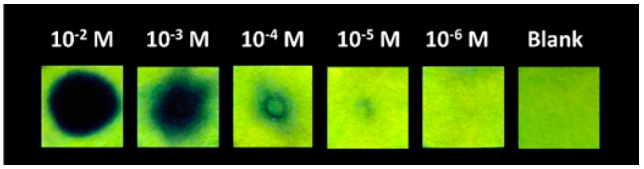

Figure 5. Photographs of portable paper strips under the UV emitting lamp of 365 nm wavelength after applying a fixed volume (10 μL) of different concentration of TNT solution.

visualized under the UV lamp up to 10 μL TNT solution (10^{-5} M), which is equivalent to 22.7 ng level and are best among the reported sensors (Table S2).

Detection of TNT in Soil Samples

To determine the ability of polymer PFPy to detect traces of TNT in natural soil samples, we collected different samples of soil from three separate locations (Figures 6 and S25).

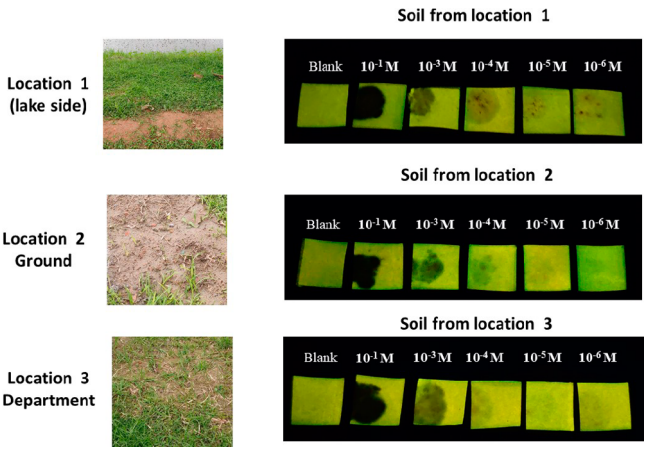

Figure 6. Photographs of three different locations and portable paper strips under UV light after being in contact with soil samples spiked with different concentration of TNT.

Thereafter, 50 mg of each soil sample was spiked with known dissimilar concentrations of 10 μL of TNT solutions. Then, PFPy coated paper strips were brought in contact with the soil samples for ∼2 min. After that, the sensing strips were examined under the UV lamp (365 nm). It could be clearly observed that the contacted portion of the paper strips with the soil samples changed to a dark spot due to the quenching process. Thus, this study confirms that the PFPy can effectively detect trace TNT quantities (22.7 ng level) present in the soil

https://doi.org/10.1021/acsmeasuresciau.1c00023
ACS Meas. Sci. Au 2022, 2, 23−30

samples. These experiments confirm that PFPy-based sensors can function both in solution as well as in a portable device for rapid on-site detection of TNT at very low concentrations, and the high sensitivity is because of the very rare multiple sensing mechanisms operating in the presence of TNT.

CONCLUSION

In summary, a newly developed cationic conjugated copolymer PFPy was successfully employed for the selective detection of TNT in parts per trillion levels in water via an intermediate Meisenheimer complex formation. This copolymeric system displayed remarkable selectivity that works even in a highly competitive environment of various interfering NACs. These extraordinary results were achieved due to the presence of a combination of both static and dynamic fluorescence quenching mechanisms, allowing a conceptually unique process of both ground-state as well as excited-state interactions of the probe PFPy with the analyte TNT that provided a very high K_S value of 26.1×10^5 M^{-1} and $K_D = 2.0 \times 10^5$ M^{-1}. PFPy also displayed instant TNT sensing ability over the economical portable paper test strip devices in contact mode and can detect as low as 22.7 ng of TNT to offer an easy, straightforward, cost-effective, and rapid sensing platform in a competitive natural environment source.

ASSOCIATED CONTENT

Supporting Information

The Supporting Information is available free of charge at https://pubs.acs.org/doi/10.1021/acsmeasuresciau.1c00023.

All the characterization data such as NMR spectra, GPC, UV−vis, and PL spectra, LoD plot, table of comparison, IFE and RET calculations, sensing photographs in solution and on paper (PDF)

AUTHOR INFORMATION

Corresponding Author

Parameswar Krishnan Iyer − *Department of Chemistry and Centre for Nanotechnology, Indian Institute of Technology Guwahati, Guwahati 781039 Assam, India;* orcid.org/0000-0003-4126-3774; Email: pki@iitg.ac.in

Authors

Arvin Sain Tanwar − *Department of Chemistry, Indian Institute of Technology Guwahati, Guwahati 781039 Assam, India;* orcid.org/0000-0003-0042-7306

Retwik Parui − *Department of Chemistry, Indian Institute of Technology Guwahati, Guwahati 781039 Assam, India*

Rabindranath Garai − *Department of Chemistry, Indian Institute of Technology Guwahati, Guwahati 781039 Assam, India;* orcid.org/0000-0002-1339-8666

Moirangthem Anita Chanu − *Department of Chemistry, Indian Institute of Technology Guwahati, Guwahati 781039 Assam, India*

Complete contact information is available at: https://pubs.acs.org/10.1021/acsmeasuresciau.1c00023

Notes

The authors declare no competing financial interest.

ACKNOWLEDGMENTS

Department of Electronics & Information Technology, (Deity) No. 5(9)/2012-NANO (Vol. II), Department of Science and Technology (DST/CRG/2019/002614), and Max-Planck-Gesellschaft (IGSTC/MPG/PG(PKI)/2011A/48) are acknowledged for financial support. Authors thank CIF for instrument facilities and CoE-SusPol, IIT Guwahati funded by the Department of Chemicals and Petrochemicals (No. 15012/9/2012-PC.1) for GPC analysis.

REFERENCES

(1) Sun, X.; Wang, Y.; Lei, Y. Fluorescence based explosive detection: from mechanisms to sensory materials. *Chem. Soc. Rev.* **2015**, *44* (22), 8019−8061.

(2) Sun, Y.; Wu, Y.; Yu, C.; Zhang, L.; Song, G.; Yao, Z. Self-Assembly of nanoscale induced excimers of 12-Pyren-1-yldodecanoic acid for TNT detection. *ACS Appl. Nano Mater.* **2019**, *2* (6), 3453−3458.

(3) Agency for toxic substances and disease registry *Toxicological profile for 2,4,6-trinitrotoluene*; 1995; https://wwwn.cdc.gov/TSP/ToxProfiles/ToxProfiles.aspx?id=677&tid=125.

(4) Hakonen, A.; Andersson, P. O.; Stenbæk Schmidt, M.; Rindzevicius, T.; Käll, M. Explosive and chemical threat detection by surface-enhanced Raman scattering: a review. *Anal. Chim. Acta* **2015**, *893*, 1−13.

(5) Zhao, X.; Yinon, J. Characterization and origin identification of 2,4,6-trinitrotoluene through its by-product isomers by liquid chromatography−atmospheric pressure chemical ionization mass spectrometry. *J. Chromatogr. A* **2002**, *946* (1), 125−132.

(6) Trammell, S. A.; Melde, B. J.; Zabetakis, D.; Deschamps, J. R.; Dinderman, M. A.; Johnson, B. J.; Kusterbeck, A. W. Electrochemical detection of TNT with in-line pre-concentration using imprinted diethylbenzene-bridged periodic mesoporous organosilicas. *Sens. Actuators, B* **2011**, *155* (2), 737−744.

(7) Soldate, A. M.; Noyes, R. M. X-Ray diffraction patterns for identification of crystalline constituents of explosives. *Anal. Chem.* **1947**, *19* (7), 442−444.

(8) Calcerrada, M.; González-Herráez, M.; García-Ruiz, C. Recent advances in capillary electrophoresis instrumentation for the analysis of explosives. *TrAC, Trends Anal. Chem.* **2016**, *75*, 75−85.

(9) Senthamizhan, A.; Celebioglu, A.; Bayir, S.; Gorur, M.; Doganci, E.; Yilmaz, F.; Uyar, T. Highly fluorescent pyrene-functional polystyrene copolymer nanofibers for enhanced sensing performance of TNT. *ACS Appl. Mater. Interfaces* **2015**, *7* (38), 21038−21046.

(10) Wu, X.; Hang, H.; Li, H.; Chen, Y.; Tong, H.; Wang, L. Water-dispersible hyperbranched conjugated polymer nanoparticles with sulfonate terminal groups for amplified fluorescence sensing of trace TNT in aqueous solution. *Mater. Chem. Front.* **2017**, *1* (9), 1875−1880.

(11) Xiao, S. J.; Zhao, X. J.; Hu, P. P.; Chu, Z. J.; Huang, C. Z.; Zhang, L. Highly photoluminescent molybdenum oxide quantum dots: one-pot synthesis and application in 2,4,6-trinitrotoluene determination. *ACS Appl. Mater. Interfaces* **2016**, *8* (12), 8184−8191.

(12) Alizadeh, N.; Akbarinejad, A.; Ghoorchian, A. Photophysical diversity of water-soluble fluorescent conjugated polymers induced by surfactant stabilizers for rapid and highly selective determination of 2,4,6-trinitrotoluene traces. *ACS Appl. Mater. Interfaces* **2016**, *8* (37), 24901−24908.

(13) Venkatramaiah, N.; Firmino, A. D. G.; Almeida Paz, F. A.; Tomé, J. P. C. Fast detection of nitroaromatics using phosphonate pyrene motifs as dual chemosensors. *Chem. Commun.* **2014**, *50* (68), 9683−9686.

(14) Yang, J.; Wang, Z.; Hu, K.; Li, Y.; Feng, J.; Shi, J.; Gu, J. Rapid and specific aqueous-Phase detection of nitroaromatic explosives with inherent porphyrin recognition sites in metal−organic frameworks. *ACS Appl. Mater. Interfaces* **2015**, *7* (22), 11956−11964.

(15) Yang, J.-S.; Swager, T. M. Fluorescent porous polymer films as TNT chemosensors: electronic and structural effects. *J. Am. Chem. Soc.* **1998**, *120* (46), 11864−11873.
(16) Nie, H.; Zhao, Y.; Zhang, M.; Ma, Y.; Baumgarten, M.; Müllen, K. Detection of TNT explosives with a new fluorescent conjugated polycarbazole polymer. *Chem. Commun.* **2011**, *47* (4), 1234−1236.
(17) Xu, B.; Wu, X.; Li, H.; Tong, H.; Wang, L. Selective detection of TNT and picric acid by conjugated polymer film sensors with donor−acceptor architecture. *Macromolecules* **2011**, *44* (13), 5089−5092.
(18) He, G.; Yan, N.; Yang, J.; Wang, H.; Ding, L.; Yin, S.; Fang, Y. Pyrene-containing conjugated polymer-based fluorescent films for highly sensitive and selective sensing of TNT in aqueous medium. *Macromolecules* **2011**, *44* (12), 4759−4766.
(19) Lee, J. Y.; Root, H. D.; Ali, R.; An, W.; Lynch, V. M.; Bähring, S.; Kim, I. S.; Sessler, J. L.; Park, J. S. Ratiometric turn-On fluorophore displacement ensembles for nitroaromatic explosives detection. *J. Am. Chem. Soc.* **2020**, *142* (46), 19579−19587.
(20) Climent, E.; Biyikal, M.; Gröninger, D.; Weller, M. G.; Martínez-Máñez, R.; Rurack, K. Multiplexed Detection of Analytes on Single Test Strips with antibody-gated indicator-releasing mesoporous nanoparticles. *Angew. Chem., Int. Ed.* **2020**, *59* (52), 23862−23869.
(21) Wan, W.-M.; Tian, D.; Jing, Y.-N.; Zhang, X.-Y.; Wu, W.; Ren, H.; Bao, H.-L. NBN-doped conjugated polycyclic aromatic hydrocarbons as an AIEgen class for extremely sensitive detection of explosives. *Angew. Chem., Int. Ed.* **2018**, *57* (47), 15510−15516.
(22) Tanwar, A. S.; Hussain, S.; Malik, A. H.; Afroz, M. A.; Iyer, P. K. Inner filter effect based selective detection of nitroexplosive-picric acid in aqueous solution and solid support using conjugated polymer. *ACS Sens.* **2016**, *1* (8), 1070−1077.
(23) Kim, H. N.; Guo, Z.; Zhu, W.; Yoon, J.; Tian, H. Recent progress on polymer-based fluorescent and colorimetric chemosensors. *Chem. Soc. Rev.* **2011**, *40* (1), 79−93.
(24) Thomas, S. W.; Joly, G. D.; Swager, T. M. Chemical sensors based on amplifying fluorescent conjugated polymers. *Chem. Rev.* **2007**, *107* (4), 1339−1386.
(25) Feng, L.; Li, H.; Qu, Y.; Lü, C. Detection of TNT based on conjugated polymer encapsulated in mesoporous silica nanoparticles through FRET. *Chem. Commun.* **2012**, *48* (38), 4633−4635.
(26) Novotney, J. L.; Dichtel, W. R. Conjugated porous polymers for TNT vapor detection. *ACS Macro Lett.* **2013**, *2* (5), 423−426.
(27) Adil, L. R.; Gopikrishna, P.; Iyer, P. K. Receptor-free detection of picric acid: a new structural approach for designing aggregation-induced emission probes. *ACS Appl. Mater. Interfaces* **2018**, *10* (32), 27260−27268.
(28) Tanwar, A. S.; Adil, L. R.; Afroz, M. A.; Iyer, P. K. Inner filter effect and resonance energy transfer based attogram level detection of nitroexplosive picric acid using dual emitting cationic conjugated polyfluorene. *ACS Sens.* **2018**, *3* (8), 1451−1461.
(29) Tanwar, A. S.; Patidar, S.; Ahirwar, S.; Dehingia, S.; Iyer, P. K. Receptor free" inner filter effect based universal sensors for nitroexplosive picric acid using two polyfluorene derivatives in the solution and solid states. *Analyst* **2019**, *144* (2), 669−676.
(30) Hussain, S.; Malik, A. H.; Afroz, M. A.; Iyer, P. K. Ultrasensitive detection of nitroexplosive − picric acid via a conjugated polyelectrolyte in aqueous media and solid support. *Chem. Commun.* **2015**, *51* (33), 7207−7210.
(31) Lakowicz, J. R. *Principles of Fluorescence Spectrosopy*, 3rd ed.; Springer: Singapore, 2010.
(32) Tanwar, A. S.; Meher, N.; Adil, L. R.; Iyer, P. K. Stepwise elucidation of fluorescence based sensing mechanisms considering picric acid as a model analyte. *Analyst* **2020**, *145* (14), 4753−4767.
(33) Xu, S.; Lu, H.; Li, J.; Song, X.; Wang, A.; Chen, L.; Han, S. Dummy Molecularly Imprinted Polymers-Capped CdTe Quantum Dots for the Fluorescent Sensing of 2,4,6-Trinitrotoluene. *ACS Appl. Mater. Interfaces* **2013**, *5* (16), 8146−8154.
(34) Zhu, H.; Zhang, H.; Xia, Y. Planar Is Better: Monodisperse Three-Layered MoS2 Quantum Dots as Fluorescent Reporters for 2,4,6-Trinitrotoluene Sensing in Environmental Water and Luggage Cases. *Anal. Chem.* **2018**, *90* (6), 3942−3949.

https://doi.org/10.1021/acsmeasuresciau.1c00023
ACS Meas. Sci. Au 2022, 2, 23−30